analytical chemistry

Article

pubs.acs.org/ac

Discrimination between 5-Hydroxymethylcytosine and 5-Methylcytosine in DNA via Selective Electrogenerated Chemiluminescence (ECL) Labeling

Shangxian Ma,[†] Huiping Sun,[†] Yan Li,[*,†] Honglan Qi,[*,‡] and Jianbin Zheng[†]

[†]Key Laboratory of Electroanalytical Chemistry of Shaanxi Province, Institute of Analytical Science, Northwest University, Xi'an, 710069, People's Republic of China

[‡]Key Laboratory of Analytical Chemistry for Life Science of Shaanxi Province, School of Chemistry and Chemical Engineering, Shaanxi Normal University, Xi'an, 710062, People's Republic of China

Supporting Information

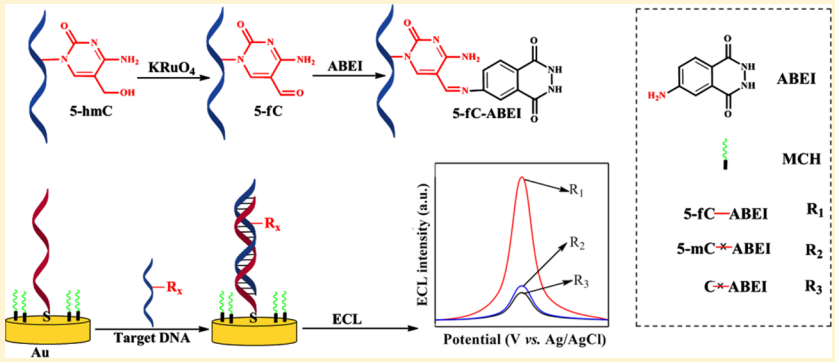

ABSTRACT: DNA methylation is used to dynamically reprogram cells in the course of early embryonic development in mammals. 5-Hydroxymethylcytosine in DNA (5-hmC-DNA) plays essential roles in the demethylation processes. 5-Methylcytosine in DNA (5-mC-DNA) is oxidized to 5-hmC-DNA by 10−11 translocation proteins, which are relatively high abundance in embryonic stem cells and neurons. A new method was developed herein to quantify 5-hmC-DNA based on selective electrogenerated chemiluminescence (ECL) labeling with the specific oxidation of 5-hmC to 5-fC by $KRuO_4$. A thiolated capture probe (ssDNA, 35-mer) for the target DNA containing 5-hmC was self-assembled on a gold surface. The 5-hmC in the target DNA was selectively transformed to 5-fC via oxidation by $KRuO_4$ and then subsequently labeled with *N*-(4-aminobutyl)-*N*-ethylisoluminol (ABEI). The ABEI-labeled target DNA was hybridized with the capture probe on the electrode, resulting in a strong ECL emission. An extremely low detection limit of 1.4×10^{-13} M was achieved for the detection of 5-hmC-DNA. In addition, this ECL method was useful for the quantification of 5-hmC in serum samples. This work demonstrates that selective 5-hmC oxidation in combination with an inherently sensitive ECL method is a promising tactic for 5-hmC biosensing.

The methylation and demethylation of cytosine (C) in DNA is a fundamental epigenetic modification present in the genomes of most plants and animals. The process has a vital function in the regulation of developmental genomic stability, X-chromosome inactivation, chromatin remodeling, genomic imprinting, and gene expression.[1−4] Aberrant DNA methylation is a well-recognized hallmark of many diseases, such as cancers, neurological disorders, diabetes, and heart disease.[5,6] The formation of 5-methylcytosine (5-mC) is well-documented.[7] Newly discovered in 2009, 5-hydroxymethylcytosine (5-hmC) is a naturally occurring nucleobase that is abundant in neurons and embryonic stem cells.[8,9] 5-Methylcytosine in DNA (5-mC-DNA) is oxidized to 5-hmC-DNA by 10−11 translocation (TET) proteins. Recently, the importance of 5-hmC was revealed in studies on DNA demethylation, behaving as a vital intermediate in the determination of replication-independent or replication-dependent demethylation.[9,10] An effective method for determining the presence and abundance of 5-hmC in DNA is required to reveal the relationship between the production of 5-hmC and the demethylation mechanism.

Single-nucleotide sequencing of 5-mC has been performed using bisulfite sequencing (BS-Seq), but this technique cannot distinguish 5-mC from 5-hmC.[11] Many strategies featuring the labeling and enrichment of 5-hmC have been employed. For instance, commercially available methods for the selective enrichment of 5-hmC with anti-5-hmC antibodies have been developed.[12] Creating affinity-enriched 5-hmC-containing DNA using a biotin tag is frequently conducted to realize base-resolution sequencing.[13−16] Although these methods can confirm the existence of 5-hmC, even in DNA samples,

Received: March 31, 2016
Accepted: September 13, 2016
Published: September 13, 2016

DOI: 10.1021/acs.analchem.6b01265
Anal. Chem. 2016, 88, 9934−9940

Scheme 1. Schematic Diagram of the ECL-Based Assay Used To Detect 5-hmC-DNA

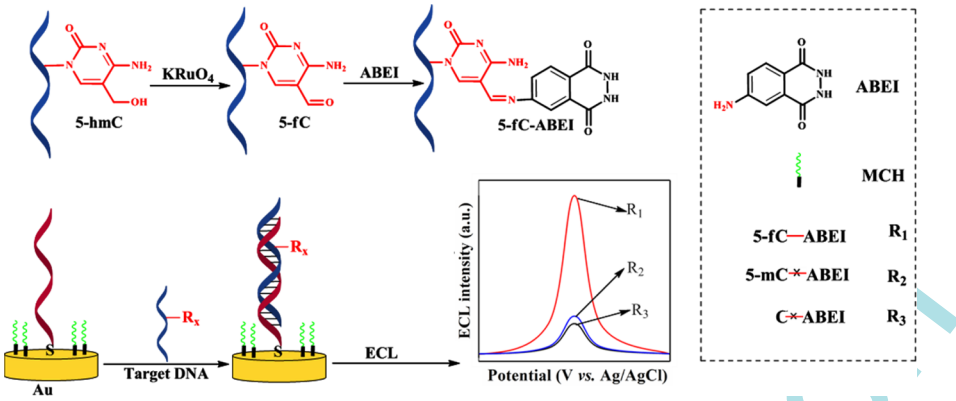

detecting whether the 5-mC in a sequence is hydroxylated or whether a specific 5-mC is hydroxylated remains difficult.

Thus, an effective chemical method for the easy detection of 5-hmC is required. In addition, developing a reaction that gives 5-hmC-positive, 5-mC-negative, and 5-C-negative results is desirable. Some methods for discriminating 5-hmC from 5-mC and 5-C involve BS-Seq and single-base resolution. Balasubramanian and co-workers reported that 5-hmC was exclusively oxidized to 5-formylcytosine (5-fC) by $KRuO_4$ in high yield[17] and that 5-hmC could be converted to U, followed by BS treatment. Therefore, the 5-hmC within genomic DNA was mapped by comparing oxidative BS-Seq with $KRuO_4$ and BS-Seq-only results. He et al. used β-glucosyltransferase to innovatively transform 5-hmC into β-glucosyl-5-hmC, which was shielded by transformation to uridine (U) after oxidization with TET mC dioxygenase (Tet 1) and BS treatment.[18,19] In fact, this direct-labeling method has many shortcomings. Compared with 5-hmC, the more active 5-fC can react with hydrazine or hydroxylamine derivatives tagged with a biotin or fluorophore moiety for subsequent determination.[14,20−24] Zhou's group discovered a method to directly label 5-fC using active amino-containing dyes or hydroxylamine.[21] These fluorescent dyes can selectively label 5-fC in high yield without a catalyst at room temperature to form a stable imine. Through this labeling reaction, the 5-fC-DNA could be identified by polyacrylamide gel electrophoresis (PAGE) or fluorescence measurements. Recently, Zhou's group reported a quantification method for the 5-hmC within genomic DNA that employs the fluorescence resonance energy transfer (CCP-FRET) assay based on a cationic conjugated polymer, in which the CCPs act as energy donors, combined with the specific oxidation of 5-hmC to 5-fC.[23]

Electrogenerated chemiluminescence (ECL) involves generating light emissions using electrochemical reactions to produce highly reactive species on an electrode, which can yield excited states in energetic electron transfer reactions upon annihilation.[25,26] In past decades, the ECL method gained wide attention for its theoretical and practical value, because of its inherent features, such as high sensitivity, low background, and good reproducibility. In this study, we developed a method for the quantification of 5-hmC within DNA via ECL, following selective oxidation. We report the first demonstration of an *N*-(4-aminobutyl)-*N*-ethylisoluminol (ABEI)-based method to detect 5-hmC based on the coupling of ABEI and 5-hmC, which is selectively oxidized to 5-fC by $KRuO_4$ in high efficiency. The underlying mechanism is depicted in Scheme 1. The procedure begins with the modification of 5-hmC covalently linked to an ECL reporter. The labeling reaction is a two-step process: (1) 5-hmC is exclusively oxidized to 5-fC by $KRuO_4$ in high efficiency, and (2) the aldehyde group is linked to the ECL species ABEI via conjugation with an amino substituent of ABEI, forming ECL-tagged 5-fC-DNA (5-fC-DNA-ABEI). Under an applied bias, this DNA product emits an ECL signal that is proportional to the number of 5-hmC residues. Thus, a significant ECL signal from the ABEI-labeled DNA is detected only if the DNA is modified by 5-fC. In comparison, no ECL is observed when the ABEI-labeled DNA is not modified by 5-fC. In this work, the proposed ECL method is discussed in detail, and the analytical performance of this technique for determining 5-hmC in DNA and discriminating between 5-hmC and 5-mC in DNA is presented.

EXPERIMENTAL SECTION

Materials and Reagents. *N*-(4-aminobutyl)-*N*-ethylisoluminol (ABEI), Tris-(2-carboxyethyl) phosphine hydrochloride (TCEP), and 6-mercapto-1-hexanol (MCH) were purchased from Sigma−Aldrich. $KRuO_4$ was obtained from Alfa Aesar (Beijing, China). The DNA sequences were purchased from Takara (China). DNA capture probe (DNA S1): 5′-HS-$(CH_2)_6$-TGC GTG CGC GCT CCC GAG TCG ACC TCC GTA GTC TT-3′; complementary DNA with one 5-hmC modification (DNA S2): 5′-AAG ACT ACG GAG GTC GAC T$^{5\text{-hm}}$CG GGA GCG CGC ACG CA-3′; complementary DNA with three 5-hmC modifications (DNA S3): 5′-AAG ACT A$^{5\text{-hm}}$CG GAG GTC GAC T$^{5\text{-hm}}$CG GGA GCG CGC A$^{5\text{-hm}}$CG CA-3′; complementary DNA with 5-mC modifications (DNA S4): 5′-AAG ACT ACG GAG GTC GAC T$^{5\text{-m}}$CG GGA GCG CGC ACG CA-3′; complementary DNA with normal cytosine as a control (DNA S5): 5′-AAG ACT ACG GAG GTC GAC TCG GGA GCG CGC ACG CA-3′; three-base-mismatch DNA (DNA S6): 5′-AAG **C**CT ACG GAG GTC G**C**C T$^{5\text{-hm}}$CG GGA GCG CGC **C**CG CA-3′; and noncomplementary DNA (DNA S7): 5′-CCT CAC CAT CTC AAG CAA ATA TAT ATT AAG $^{5\text{-hm}}$CGT AT-3′. The 35-mer target ssDNA (DNA S2), corresponding to portions of the *Homo sapiens* von Hippel−Lindau tumor suppressor (VHL) segment (accession No. JX401534, the sequence was submitted to BLAST at http://blast.st-va.ncbi.nlm.nih.gov/Blast.cgi), was adopted from ref 23. The seven-oligonucleotide solution was prepared using Tris-ethylenediaminetetraacetic acid (EDTA) (TE) buffer (10 mM Tris, 1 mM EDTA, pH 8.0) in the desired concentrations and stored at −20 °C. The other reagents were

DOI: 10.1021/acs.analchem.6b01265
Anal. Chem. 2016, 88, 9934−9940

used as received, without further purification. All solutions were prepared with Millipore Milli-Q water (18.2 MΩ cm).

The ECL experiments were conducted with an MPI-A ECL detector (Xi'an Remax Electronics, China). Specifically, ECL was detected by a photomultiplier tube (PMT) that was biased at −900 V throughout the work. A traditional three-electrode configuration was employed, in which a gold electrode (2.0 mm diameter) functioned as the working electrode, a Ag/AgCl (saturated KCl) electrode functioned as the reference electrode, and a platinum wire functioned as the counter electrode. All electrochemical measurements, including electrochemical impedance spectroscopy (EIS) and cyclic voltammetry (CV), were conducted using a CHI Model 660 potentiostat (Chenhua Instruments, Shanghai). Atomic force microscopy (AFM) images were obtained with a scanning probe microscope (Model CSPM5500, Beijng Nano-Instruments, Ltd., China; http://www.gongchang.com). High-performance liquid chromatography (HPLC) measurements were performed on a LC-10Avp Plus instrument (Shimadzu Corporation, Japan). The ultraviolet−visible (UV-vis) absorption and fluorescence spectra were recorded on a UV-vis spectrophotometer (Model UV-2450, Shimadzu Corporation, Japan).

ssDNA Oxidation by $KRuO_4$ and ABEI Labeling of 5-fC-Containing DNA. The optimized experimental procedure is described as follows. Two hundred microliters (200 μL) of DNA S2 (1 μM) was added to 10 μL of $KRuO_4$ (100 μM). The reaction was performed in a 0 °C ice water bath for 1 h to afford 5-fC DNA. Excess $KRuO_4$ was removed through MF-Millipore membranes, followed by a dialysis membrane. After the 40 μL of ABEI (100 μM) was introduced, the solution was placed in water bath at 37 °C for 12 h. The excess ABEI was removed using standard ethanol precipitation, which was performed twice. The total yield exceeded 90%.

Polyacrylamide Gel Electrophoresis (PAGE) of ECL-Labeled DNA. The DNAs containing different modifications were oxidized by $KRuO_4$ and then labeled by ABEI following the procedure described above. A total of 800 μL of ethanol and 10 μL of CH_3COONa-CH_3COOH buffer (1 M, pH 5.0) were then added to the ECL-labeled DNA solution. Finally, the mixture was frozen for 2 h at −80 °C, followed by centrifugation (10 000 rpm) for 20 min at 4 °C. The DNAs were then loaded into a 20% polyacrylamide gel for electrophoresis at 20 V/cm in 1 × TBE (Tris/borate/EDTA) buffer at room temperature.

Preparation of the Biosensing Electrode. The gold disk electrode was polished with a 0.3 μm alumina slurry (Beuhler) and then ultrasonicated in water for 5 min. The resulting electrode was electrochemically cleaned by scanning the potential between 0 and +1.5 V in 0.10 M H_2SO_4 until the faradic current was not clearly observed.[27,28] The cleaned gold electrode was immersed in 100 μL of a 1 μM DNA S1 solution (in TE buffer: 10 mM Tris, 1.0 mM EDTA, 1.0 M NaCl, 1.0 mM TCEP, pH 7.0) and incubated for 4 h at 37 °C. The modified electrode was washed with buffer (10 mM Tris, pH 7.4) and water to clean the nonspecifically adsorbed DNA S1. The modified electrode was immersed in a 1 mM MCH solution for 1 h to block the uncovered surface of the electrode. The obtained DNA S1-self-assembled gold electrode was then thoroughly rinsed with buffer (10 mM Tris, pH 7.4) and employed as the ECL biosensing electrode.

ECL Measurements. The DNA S1-self-assembled electrode was dipped in 100 μL of 10 mM Tris (pH 7.4) containing 5-fC-DNA-ABEI or a serum sample for 2 h at 37 °C and was then cleaned with water. The ECL experiments were conducted using a triangular potential scan at 100 mV s^{-1} in 0.10 M phosphate-buffered saline (pH 7.4) comprising 1 mM H_2O_2.[29] The 5-hmC-DNA content was quantified based on the ECL intensity at +700 mV.

RESULTS AND DISCUSSION

ECL Labeling of 5-fC-DNA. Because $KRuO_4$ is highly soluble in water, it can easily oxidize 5-hmC-DNA to 5-fC-DNA in high yields.[24] The efficiency of this oxidation for the target DNA in this work was demonstrated by HPLC (~95% yield; see Figures S1 and S2 in the Supporting Information). Figure 1 shows the results of PAGE analysis of ECL-labeled DNA with different modifications, and the relative positions are according to their molecular weights. Lanes 1, 2, and 3 represent the oxidation-label reaction of DNA S5 (C-DNA), DNA S4 (5-mC-DNA), and DNA S2 (5-hmC-DNA), respectively. The right image of Figure 1 was taken under 254 nm UV light. The absence of a fluorescence band in lanes 1 and 2 indicates that normal bases and 5-mC cannot be oxidized; therefore, ABEI cannot react with these bases in DNA S4. The DNA S2 fluorescence band appears in lane 3. Thus, 5-hmC can be selectively oxidized by $KRuO_4$ and subsequently labeled by ABEI. Figure S3 in the Supporting Information shows that the HPLC retention time of 5-fC-DNA is in agreement with previously reported values.[23] Both PAGE and HPLC indicate that the oxidation and labeling reactions have very high yields (>90%). UV-vis absorption spectroscopy was also used to characterize the interaction between 5-fC-DNA and ABEI. Figure 2 shows the absorption spectra of 5-fC-DNA, ABEI, and the 5-fC-DNA-ABEI composite. 5-fC-DNA displays an obvious absorption peak at ~284 nm, whereas ABEI exhibits a peak at 240 nm. The 5-fC-DNA-ABEI composite shows peaks at 284 and 240 nm that correspond to the absorption spectra of 5-fC-DNA and ABEI, respectively. These results indicate that 5-

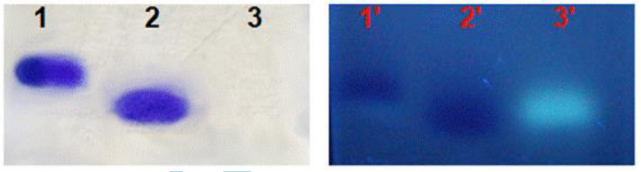

Figure 1. PAGE analysis (20%, denatured gels) of different DNAs oxidized by $KRuO_4$ and then labeled with ABEI under the same conditions. Lanes 1, 2, and 3 represent C-DNA, 5-mC-DNA, and 5-hmC-DNA, respectively. The gel was excited by visible light (left) and UV light (right, 254 nm).

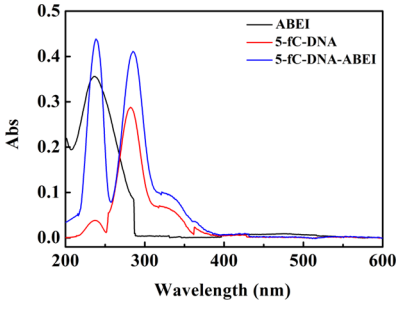

Figure 2. UV-vis absorption spectra of ABEI (black line), 5-fC-DNA (red line), and a 5-fC-DNA-ABEI composite (blue line).

DOI: 10.1021/acs.analchem.6b01265
Anal. Chem. 2016, 88, 9934−9940

fC-DNA was labeled with ABEI; the characteristic absorption peaks were identified through comparison with previously reported literature values.[30,31] These results are in good agreement with the PAGE analysis.

Immobilization of DNA on Gold Surfaces. X-ray photoelectron spectroscopy (XPS) was performed to characterize the self-assembled the capture-prone DNA S1 onto the gold surfaces.[32] Figure 3A shows the XPS spectra of the N(1s) peaks

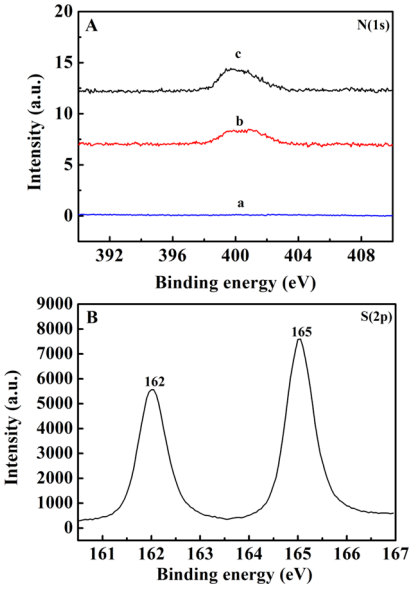

Figure 3. (A) XPS spectra of the N(1s) peak of a gold surface: without oligonucleotide (spectrum a), with 1 μM DNA S1 (spectrum b), and after hybridization of DNA S1 with DNA S2 (spectrum c). The intensities were normalized to the corresponding Au(4f) emission. (B) XPS spectra of the S(2p) peak of a gold surface.

from different DNA sequences. Curve a in Figure 3A shows the absence of an N(1s) signal peak, implying a deficiency of the oligonucleotide on the bare gold surface. For the gold plates self-assembled with DNA S1 and the hybridization of the self-assembled DNA S1 with DNA S2, N(1s) peaks are featured in curves b and c in Figure 3A, respectively. The hybridization process (*vide infra*) probably results in an increase in the area of the N(1s) peak of 66.67%, indicating successful self-assembly and hybridization. In the XPS simulation, the two main constituents, including the Au−S bound (162 eV) and unbounded S (165 eV, Figure 3B) indicated that DNA S1 had self-assembled onto the gold surface through Au−S bonding, S(2p) (162 eV).

The AFM measurements were used to characterize the topography of the gold surfaces self-assembled by the captured DNA S1 and then hybridized with DNA S2 on the surfaces. Figure 4A displays an AFM image (703 nm × 703 nm) of the bare gold surface. The bare gold surface was characterized by separated large-area terraces. A textured morphology was observed for the DNA S1 self-assembling gold surface (Figure 4B) and the DNA S1 self-assembling gold surface after hybridization with DNA S2. Figure 4C shows a similar textured morphology, but a more globular morphology with an increasing average size of ~124 nm was observed on the DNA S1 self-assembling gold surface after hybridization with DNA S2. Figure 4D represents the typical linear scans associated with Figures 4B and 4C. The average apparent size of the immobilized DNA S1 was ~80 nm, suggesting the loss of

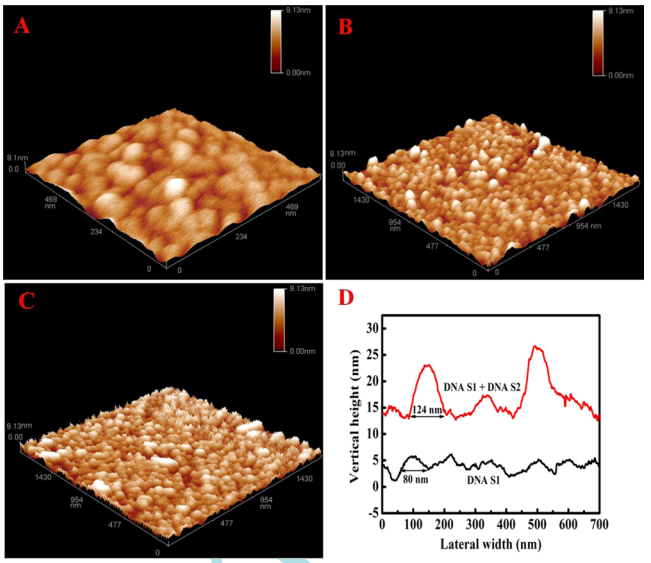

Figure 4. Contact-mode AFM image of (A) a bare Au single-crystal surface (image size: 703 nm × 703 nm); (B) Au surface after self-assembly with DNA S1 (image size: 1907 nm × 1907 nm); (C) Au surface after self-assembly with DNA S1 that was subsequently hybridized with DNA S2 (image size: 1907 nm × 1907 nm); and (D) linear scans associated with panel B (lower curve) and panel C (upper curve).

its linear shape and crinkling into small globular aggregates. After DNA S1 had hybridized with DNA S2, the average apparent size increased to ~124 nm. The increase in the lateral average size of the globular texture was mainly ascribed to the hybridization of DNA S1 with DNA S2.[33]

Electrochemical Characterization of the Biosensing Electrode. EIS and CV were performed to monitor the fabrication of the biosensing electrode. Figure S4A in the Supporting Information shows the Nyquist plots of the impedance spectra collected with different electrodes. An equivalent circuit model (inset in Figure S4A) was used to fit the results. This circuit includes the charge-transfer resistance (R_{ct}), the ohmic resistance of the electrolyte solution (R_s), the Warburg impedance (Z_w), and the interface capacitance (C).[34] The experimental impedance data were in agreement with the data (red line) fitted with commercial software (CHI, Model 660) (Figure S4A). The diameter of the semicircle corresponds to R_{ct}. Figure S4A shows that the bare gold electrode (curve a) exhibited a very small semicircle diameter, suggesting a low charge-transfer resistance (R_{ct} = 110 Ω). When DNA S1 and MCH were self-assembled on the gold electrode, the value of R_{ct} increased to 2937 Ω, which is likely a result of the electrostatic repulsion between the negatively charged DNA self-assembled on the gold electrode and the $Fe(CN)_6^{3-/4-}$ in solution.[35] After the DNA S1 self-assembled electrode was hybridized with DNA S2 (5-hmC-DNA), R_{ct} increased to 5687 Ω (curve d in Figure S4A). Therefore, DNA S1 was demonstrated to be successfully fixed on the electrode, forming a sensing interface. The CV results (Figure S4B) were consistent with the results from the impedance experiments, providing further evidence of the successful immobilization of DNA S1 on the gold electrode surface, with subsequent hybridization of DNA S1 and DNA S2.

Feasibility Study. Figure 5 demonstrates the corresponding ECL profiles of DNA S1 hybridized with different DNAs (DNA S2, DNA S3, DNA S4, DNA S5, DNA S6, and DNA S7)

DOI: 10.1021/acs.analchem.6b01265
Anal. Chem. 2016, 88, 9934−9940

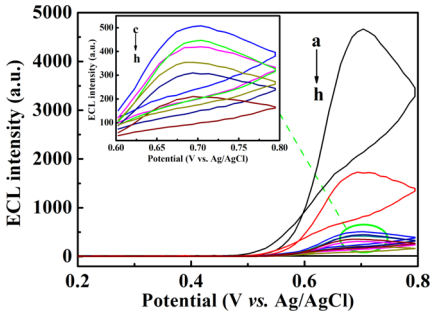

Figure 5. ECL intensity vs potential profiles for different DNAs combined with ABEI; the concentration of all DNAs was 1.0×10^{-11} M: 5-hmC-DNA (DNA S3) after oxidization (line a), 5-hmC-DNA (DNA S2) after oxidization (line b), 5-hmC-DNA (DNA S2) without oxidization (line c), three-base mismatch DNA (DNA S6) after oxidization (line d), 5-mC-DNA (DNA S4) after oxidization (line e), noncomplementary DNA (DNA S7) after oxidization (line f), C-DNA (DNA S5) after oxidization (line g), and hybridization buffer without DNA (line h). (Measurement conditions: 0.1 M PBS containing 1 mM H_2O_2, pH 7.4; scan rate, 100 mV/s.)

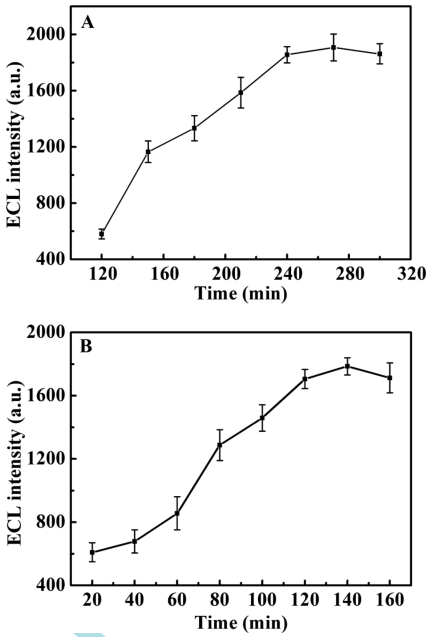

Figure 6. (A) Effect of self-assembly time on the ECL intensity for 1.0×10^{-6} M DNA S1; (B) effect of hybridization time on the ECL intensity for 1.0×10^{-11} M 5-hmC-DNA (DNA S2).

that had been labeled with ABEI. The ECL mechanism of ABEI is similar to that of luminol, and the oxidation product is possibly diazabenzoquinone.[36] Diazabenzoquinone is transformed to hydroperoxide or endoperoxide by H_2O_2, and the excited state of aminophthalic acid is generated by splitting the diazabenzoquinone ring, along with the emission of luminescence. Compared with that of line b in Figure 5, the increase ratio of the ECL intensity (line a in Figure 5) was ~300% at the same concentration, because the number of 5-hmC sites in DNA S3 (three 5-hmC sites) was higher than that in DNA S2 (one 5-hmC site). This result indicates that the ECL intensity was correlated with the level of DNA hydroxymethylation. Slight ECL intensity changes were observed in other tested DNA sequences, including DNA S4, DNA S5, and unoxidized DNA S2—but were almost equivalent to that of the blank measurement (hybridization buffer without DNA), because the 5-mC sites in DNA S4 and 5-C sites in DNA S5 could not be selectively transformed to 5-fC via oxidation by $KRuO_4$ and were not subsequently labeled with ABEI. The 5-hmC in unoxidized DNA S2 was not labeled by ABEI. In addition, three mismatched sequences (DNA S6) and a noncomplementary sequence (DNA S7) were selected to evaluate the selectivity of this method. Compared with line h in Figure 5, the ECL intensity (lines d and f in Figure 5) remained almost constant, because DNA S6 and DNA S7 did not efficiently hybridize with the capture probe DNA S1 immobilized on the gold electrode, respectively. These results indicate that the developed method has good selectivity for even three-base mismatched 5-hmC-DNA and could be applied to analyze 5-hmC-DNA.

Detection Condition Optimization. Figure 6A shows the effect of the self-assembly time on the ECL signal intensity. The ECL intensity increased abruptly with the increase in the self-assembled time over a range between 120 and 240 min. A maximum in the ECL intensity was reached at 270 min, after which the steric and electrostatic effects gradually dominated to slightly decrease the ECL intensity while presenting a more tightly packed HS-DNA monolayer.[37] Therefore, 240 min was selected as the self-assembly time for the reported experiments to obtain high sensitivity and shorten the fabrication time for the biosensing electrode. Figure 6B shows the effect of the hybridization time between DNA S1 and DNA S2 on the ECL signal intensity. The ECL intensity increased abruptly with the increase in the hybridization time over a range between 20 and 120 min and then plateaued at a stable value. Therefore, the hybridization occurred within 120 min. The slower hybridization kinetic for DNA S1−DNA S2 could partially result from the lower concentration of DNA S2 (1.0×10^{-11} M) used in the experiment.[37] To ensure complete hybridization at lower DNA S2 concentrations, 140 min was set as the hybridization time.

Linear Range and Detection Limit. Figure 7 demonstrates the ECL responses as a function of the DNA S2 concentration under the optimized conditions (Figure 7A) and the calibration curve of DNA S2 (Figure 7B). Figure 7A clearly shows that the ECL signal gradually increased when the DNA S2 concentration increased from 5.0×10^{-13} to 5.0×10^{-10} M. In addition, the ECL signal intensity was proportional to the DNA S2 concentration from 5.0×10^{-13} to 1.0×10^{-10} M (Figure 7B). The linear regression equation is

$$I_{ECL} = 77.264C + 865.076$$

and the regression coefficient is 0.9954. The detection limit was calculated to be 1.4×10^{-13} M (signal-to-noise ratio (S/N) of 3). Mainly because of ABEI's excellent ECL properties, the sensitivity of this method is much higher than those of previously reported methods (see Table S1 in the Supporting Information). The detection limit of the proposed ECL biosensing method is much lower than those achieved by electrochemical approaches (1.43×10^{-12} M and 1.6×10^{-10} M),[38,39] CE-MS/MS analysis (1.0×10^{-10} M)[40] and a fluorescence approach (1.0×10^{-8} M).[23] Furthermore, our method has a detection limit that is 3-fold lower than that reported for an optical sensor (4.2×10^{-13} M)[41] and is well below the normal levels found in human urine samples (22.6 ± 13.7 nM).[40] The relative standard deviation (RSD) for 10 replicate determinations of DNA S2 at 1.0×10^{-11} M with different electrodes from the same batch was 4.32%, which

DOI: 10.1021/acs.analchem.6b01265
Anal. Chem. 2016, 88, 9934−9940

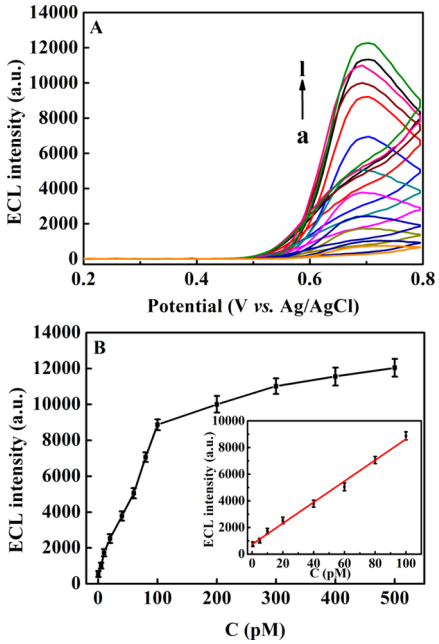

Figure 7. (A) ECL responses to different concentrations of 5-hmC-DNA (DNA S2) combined with ABEI in 0.10 M PBS (pH 7.4) containing 1 mM H_2O_2: 5.0×10^{-13} M (line a), 5.0×10^{-12} M (line b), 1.0×10^{-11} M (line c), 2.0×10^{-11} M (line d), 4.0×10^{-11} M (line e), 6.0×10^{-11} M (line f), 8.0×10^{-11} M (line g), 1.0×10^{-10} M (line h), 2.0×10^{-10} M (line i), 3.0×10^{-10} M (line j), 4.0×10^{-10} M (line k), and 5.0×10^{-10} M (line l). (B) Relationship between the ECL intensity and DNA S2 concentration. Inset: calibration curve for DNA S2 detection. Measurement conditions were the same as those described in Figure 5.

indicates good reproducibility. Therefore, the ECL method reported here shows high sensitivity and good reproducibility.

Detection of 5-hmC-DNA in Serum Samples. The effectiveness of this ABEI-based ECL method was validated by determining 5-hmC-DNA in clinical use, using human serum samples obtained from the Hospital of Shaanxi Normal University as an example. 5-hmC-DNA-spiked serum sample solutions were prepared by adding 5-hmC-DNA to final concentrations of 10, 40, and 80 pM in 100-fold diluted serum samples. The recoveries of 5-hmC-DNA in these spiked serum samples were obtained from the calibration curve (Figure 7B) presented in Table 1. The average recovery was 94.6% with

Table 1. Recovery Determination of 5-hmC-DNA in 100-Fold-Diluted Serum Samples

added amount (pM)	determined amount (pM)	recovery (%)	average recovery (%)
10.0	9.0	89.8	
40.0	41.6	103.9	94.6
80.0	72.0	90.0	

RSDs of 3.78%, 4.61%, and 3.97%, respectively. These results indicate that the developed method has potential for use with serum samples. However, the ECL biosensing method in this work only applied to detect specific target 5-hmC-ssDNA, which has been identified by DNA sequence analysis. The dsDNA and long-stranded DNA in biological and clinical samples can be detected by denaturing duplex DNA into ssDNA under certain reaction conditions or designing a capture DNA probe that is complementary to a known long-stranded DNA sequence.

CONCLUSION

A new method was developed for the quantification of 5-hmC based on an electrogenerated chemiluminescence (ECL) assay combined with the specific oxidation of 5-hmC to 5-fC. The developed method exhibited high specificity, because the chemical reaction targeting 5-hmC modifications cannot occur with nonhydroxymethylated DNA bases. As a proof-of-concept investigation, this study also showed that the developed method has a high detection sensitivity with an extremely low detection limit of 1.4×10^{-13} M for 5-hmC-DNA. The detection of 5-hmC-DNA in serum samples demonstrates that the proposed ECL strategy is characterized by high sensitivity and selectivity for this purpose. Coupling of the proposed method with a commercial ECL kit will be evaluated in point-of-care testing for other DNA mutations in future studies.

ASSOCIATED CONTENT

Supporting Information

The Supporting Information is available free of charge on the ACS Publications website at DOI: 10.1021/acs.analchem.6b01265.

HPLC chromatograms and normalized intensities of 5-hmC-DNA before and after oxidation (Figures S1 and S2); HPLC retention time of 5-fC-DNA (Figure S3); EIS and CV monitoring of the fabrication of the biosensing electrode (Figure S4); and detection limits of 5-hmC by different methods (Table S1) (PDF)

AUTHOR INFORMATION

Corresponding Authors

*Tel.: +86-29-88303448. Fax: +86-29-88303448. E-mail: yanli@nwu.edu.cn.

*Tel.: +86-29-81530726. Fax: +86-29-81530727. E-mail: honglanqi@snnu.edu.cn.

Notes

The authors declare no competing financial interest.

ACKNOWLEDGMENTS

We acknowledge the support from the National Science Foundation of China (Nos. 21375102, 21005061, and 21522504), Natural Science Basic Research Plan in Shaanxi Province of China (Nos. 2012KJXX-25 and 2016JM202) and Science and Technology Plan Project of Xi'an (No. CXY1441(8)).

REFERENCES

(1) Laird, P. W. *Nat. Rev. Cancer* **2003**, *3*, 253.
(2) Li, E. *Nat. Rev. Genet.* **2002**, *3*, 662−673.
(3) Ushijima, T. *Nat. Rev. Cancer* **2005**, *5*, 223.
(4) Frigola, J.; Song, J.; Stirzaker, C.; Hinshelwood, R. A.; Peinado, M. A.; Clark, S. J. *Nat. Genet.* **2006**, *38*, 540.
(5) Scarano, M. I.; Strazzullo, M.; Matarazzo, M. R.; D'Esposito, M. J. *J. Cell. Physiol.* **2005**, *204*, 21−35.
(6) Robertson, K. D. *Nat. Rev. Genet.* **2005**, *6*, 597−610.
(7) Jones, P. A. *Nat. Rev. Genet.* **2012**, *13*, 484−492.
(8) Kriaucionis, S.; Heintz, N. *Science* **2009**, *324*, 929−930.
(9) Tahiliani, M.; Koh, K. P.; Shen, Y.; Pastor, W. A.; Bandukwala, H.; Brudno, Y.; Agarwal, S.; Iyer, L. M.; Liu, D. R.; Aravind, L.; Rao, A. *Science* **2009**, *324*, 930−935.

DOI: 10.1021/acs.analchem.6b01265
Anal. Chem. 2016, 88, 9934−9940

(10) Gu, T. P.; Guo, F.; Yang, H.; Wu, H. P.; Xu, G. F.; Liu, W.; Xie, Z. G.; Shi, L.; He, X.; Jin, S. G.; Iqbal, K.; Shi, Y. G.; Deng, Z.; Szabo, P. E.; Pfeifer, G. P.; Li, J.; Xu, G. L. *Nature* **2011**, *477*, 606−610.
(11) Huang, Y.; Pastor, W. A.; Shen, Y.; Tahiliani, M.; Liu, D. R.; Rao, A. *PLoS One* **2010**, *5*, e8888.
(12) Ito, S.; D'Alessio, A. C.; Taranova, O. V.; Hong, K.; Sowers, L. C.; Zhang, Y. *Nature* **2010**, *466*, 1129.
(13) Song, C.-X.; Szulwach, K. E.; Fu, Y.; Dai, Q.; Yi, C.; Li, X.; Li, Y.; Chen, C.-H.; Zhang, W.; Jian, X.; Wang, J.; Zhang, L.; Looney, T.; Zhang, B.; Godley, L. A.; Hicks, L. M.; Lahn, B. T.; Jin, P.; He, C. *Nat. Biotechnol.* **2011**, *29*, 68.
(14) Pastor, W. A.; Huang, Y.; Henderson, H. R.; Agarwal, S.; Rao, A. *Nat. Protoc.* **2012**, *7*, 1909−1917.
(15) Song, C. X.; Clark, T. A.; Lu, X. Y.; Kislyuk, A.; Dai, Q.; Turner, W. S.; He, C.; Korlach, J. *Nat. Methods* **2011**, *9*, 75.
(16) Liutkeviciute, Z.; Kriukiene, E.; Grigaityte, I.; Masevicius, V.; Klimasauskas, S. *Angew. Chem., Int. Ed.* **2011**, *50*, 2090.
(17) Booth, M. J.; Branco, M. R.; Ficz, G.; Oxley, D.; Krueger, F.; Reik, W.; Balasubramanian, S. *Science* **2012**, *336*, 934−937.
(18) Yu, M.; Hon, G. C.; Szulwach, K. E.; Song, C. X.; Zhang, L.; Kim, A.; Li, X.; Dai, Q.; Shen, Y.; Park, B.; Min, J. H.; Jin, P.; Ren, B.; He, C. *Cell* **2012**, *149*, 1368.
(19) Schuler, P.; Miller, A. K. *Angew. Chem., Int. Ed.* **2012**, *51*, 10704.
(20) Raiber, E. A.; Beraldi, D.; Ficz, G.; Burgess, H. E.; Branco, M. R.; Murat, P.; Oxley, D.; Booth, M. J.; Reik, P.; Balasubramanian, S. *Genome Biol.* **2012**, *13*, R69.
(21) Guo, P.; Yan, S.; Hu, J.; Xing, X.; Wang, C.; Xu, X.; Qiu, X.; Ma, W.; Lu, C.; Weng, X.; Zhou, X. *Org. Lett.* **2013**, *15*, 3266.
(22) Hu, J.; Xing, X.; Xu, X.; Wu, F.; Guo, P.; Yan, S.; Xu, Z.; Xu, J.; Weng, X.; Zhou, X. *Chem.—Eur. J.* **2013**, *19*, 5836.
(23) Hong, T.; Wang, T.; Guo, P.; Xing, X.; Ding, F.; Chen, Y.; Wu, J.; Ma, J.; Wu, F.; Zhou, X. *Anal. Chem.* **2013**, *85*, 10797−10802.
(24) Hu, J.; Chen, Y.; Xu, X.; Wu, F.; Xing, X.; Xu, Z.; Xu, J.; Weng, X.; Zhou, X. *Bioorg. Med. Chem. Lett.* **2014**, *24*, 294−297.
(25) Miao, W. *Chem. Rev.* **2008**, *108*, 2506−2553.
(26) Liu, Z.; Qi, W.; Xu, G. *Chem. Soc. Rev.* **2015**, *44*, 3117−3142.
(27) Sun, B.; Qi, H.; Ma, F.; Gao, Q.; Zhang, C.; Miao, W. *Anal. Chem.* **2010**, *82*, 5046−5052.
(28) Shan, M.; Li, M.; Qiu, X. Y.; Qi, H. L.; Gao, Q.; Zhang, C. X. *Gold Bull.* **2014**, *47*, 57−64.
(29) Qi, H. L.; Li, M.; Dong, M. M.; Ruan, S. P.; Gao, Q.; Zhang, C. X. *Anal. Chem.* **2014**, *86*, 1372−1379.
(30) Liu, D. Q.; Huang, G. M.; Yu, Y. Q.; He, Y.; Zhang, H. L.; Cui, H. *Chem. Commun.* **2013**, *49*, 9794−9796.
(31) Murata-Kamiya, N.; Kamiya, H.; Karino, N.; Ueno, Y.; Kaji, H.; Matsuda, A.; Kasai, H. *Nucleic Acids Res.* **1999**, *27*, 4385−4390.
(32) Petrovykh, D. Y.; Kimura-Suda, H.; Whitman, L. J.; Tarlov, M. J. *J. Am. Chem. Soc.* **2003**, *125*, 5219−5226.
(33) Casero, E.; Darder, M.; Diaz, D. J.; Pariente, F.; Martin-Gago, J. A.; Abruna, H.; Lorenzo, E. *Langmuir* **2003**, *19*, 6230−6235.
(34) Patolsky, F.; Zayats, M.; Katz, E.; Willner, I. *Anal. Chem.* **1999**, *71*, 3171−3180.
(35) Radi, A. E.; Acero Sanchez, J. L.; Baldrich, E.; O'Sullivan, C. K. *Anal. Chem.* **2005**, *77*, 6320−6323.
(36) Arai, K.; Takahashi, K.; Kusu, F. *Anal. Chem.* **1999**, *71*, 2237−2240.
(37) Zhang, J.; Qi, H.; Li, Y.; Yang, J.; Gao, Q.; Zhang, C. *Anal. Chem.* **2008**, *80*, 2888−2894.
(38) Zhou, Y.; Yang, Z.; Li, X.; Wang, Y.; Yin, H.; Ai, S. *Electrochim. Acta* **2015**, *174*, 647−652.
(39) Yang, Z.; Shi, Y.; Liao, W.; Yin, H.; Ai, S. *Sens. Actuators, B* **2016**, *223*, 621−625.
(40) Yuan, F.; Zhang, X.; Nie, J.; Chen, H.; Zhou, Y.; Zhang, X. *Chem. Commun.* **2016**, *52*, 2698−2700.
(41) Hawk, R. M.; Armani, A. M. *Biosens. Bioelectron.* **2015**, *65*, 198−203.

DOI: 10.1021/acs.analchem.6b01265
Anal. Chem. 2016, 88, 9934−9940